2006

Growth optimization and structural analysis for ferromagnetic Mn-doped ZnO layers deposited by radio frequency magnetron sputtering

M. Abouzaid
CNRS-ENSICAEAN

P. Ruterana
CNRS-ENSICAEAN

C. Liu
Virginia Commonwealth University

H. Morkoç
Virginia Commonwealth University

Abouzaid, M., Ruterana, P., Liu, C., et al. Growth optimization and structural analysis for ferromagnetic Mn-doped ZnO layers deposited by radio frequency magnetron sputtering. Journal of Applied Physics 99, 113515 (2006).

Growth optimization and structural analysis for ferromagnetic Mn-doped ZnO layers deposited by radio frequency magnetron sputtering

M. Abouzaid and P. Ruterana[a)]
SIFCOM UMR 6176 CNRS-ENSICAEN, 6 Boulevard du Marechal Juin, 14050 Caen Cedex, France

C. Liu[b)] and H. Morkoç
Department of Electrical Engineering, Virginia Commonwealth University, Richmond Virginia 23284

(Received 3 January 2006; accepted 28 March 2006; published online 6 June 2006)

The effect of the deposition temperature on the crystalline quality of (Zn,Mn)O is investigated in thin films prepared by radio frequency magnetron sputtering on *c*-plane sapphire and GaN substrates. The layers are made of a 0.5 μm Mn-doped layer towards the surface on top of a 150 nm pure ZnO buffer. Depending on the deposition temperature, the layers can exhibit a columnar structure; the adjacent domains are rotated from one another by 90°, putting $[10\bar{1}0]$ and $[1\bar{1}20]$ directions face to face. At high Mn concentration the columnar structure is blurred by the formation of Mn rich precipitates. Only one variety of domains is observed at an optimal deposition temperature of 500 °C: they are slightly rotated around the [0001] axis (mosaic growth) and bounded by threading dislocations. © *2006 American Institute of Physics*.
[DOI: 10.1063/1.2200768]

I. INTRODUCTION

Semiconductors doped with magnetic ions have been extensively studied since the reports on carrier-induced ferromagnetism in In(Mn)As (Ref. 1) and later on Ga(Mn)As.[2] The calculations of Dietl *et al.* based on the Zener model of ferromagnetism predicted that Mn-doped GaN and ZnO can have a Curie Temperature T_C higher than room temperature.[3] Subsequently, considerable effort has been focused on achieving reliable ZnO-based dilute magnetic semiconductors (DMSs) with a Curie temperature above room temperature by doping with transition metals, especially Mn (Refs. 4 and 5) and Co.[6] However, the situation is still complicated as ferromagnetism has been reported in insulating Zn(Mn)O,[7] *n*-type Zn(Mn)O,[5] and *p*-type Zn(Mn)O,[8] as well as paramagnetism.[9] In addition, doping ZnO layers with these transition metal atoms may lead to the formation of various interphase precipitates, which may have magnetic properties.[10] A number of thin film deposition techniques are now available for the production of good quality ZnO layers, with pulsed laser deposition[11] (PLD) being probably one of the most used methods for this material. Metal organic chemical vapor deposition[12–14] (MOCVD) is an alternative technique for growth that has advantages such as its chemistry and thermodynamic dependent growth, control at the atomic level, large area deposition, and the possibility of different *in situ* doping processes. Typical growth conditions are as follows: chamber pressure of 20–50 Torr and growth temperature of 250–600 °C.[15] Such ZnO layers grown on sapphire were shown to have a relatively low thermal stability after annealing at about 800 °C.[15] Molecular beam epitaxy (MBE) technique is also currently used for the growth of high quality ZnO, but high dose *p* doping may be difficult.[16] It is claimed that in ZnO, ferromagnetism may be connected with *p* doping, especially using nitrogen. One of the easiest and low cost methods for introducing high doses of nitrogen may be the deposition by radio frequency (rf) magnetron sputtering.[17] For this technique incorporation of nitrogen is done directly in the plasma and large amounts may be incorporated in the layer in contrast with the other growth techniques such as MBE or PLD. However, the deposited layers may be of poorer crystalline quality and the existence of structural imperfections can impede the clarification of experimentally observed ferromagnetism in DMSs. Therefore, our aim is to develop a better understanding of the observed magnetic behavior by carrying out a detailed microstructural analysis of transition metal and nitrogen-doped ZnO thin films. In this transmission electron microscopy investigation, it is pointed out that the substrate temperature during deposition plays an important role on the layer microstructure.

II. EXPERIMENT

The ZnO buffer layer and the Mn-doped ZnO film were deposited between 500 and 750 °C. A rf power of 150 W was used to sputter the ZnO target. The dc power applied to the Mn target was 5 W for the Mn-doped ZnO film. The targets were presputtered for 5 min before the actual deposition to remove contamination from the target surface. The substrates were either sapphire or thick GaN buffer layers. The as-deposited films on sapphire substrates were annealed at 850 °C for 1 h in an air ambient in order to improve the crystalline quality. The deposition conditions are summarized in Table I.

Cross sectional transmission electron microscopy (TEM) samples were prepared by gluing two pieces of the film face to face, cutting to slices, followed by mechanical polishing

[a)]Author to whom correspondence should be addressed; FAX: +33 2 31 45 26 60; electronic mail: pierre.ruterana@ensicaen.fr
[b)]Present address: School of Physics, Seoul National University, Seoul 151-747, Korea.

TABLE I. Deposition temperature, substrate, and doping of the investigated samples.

Sample	Substrate	T (°C)	N (SCCM)
SP105	Sapphire	550	0
SP110	Sapphire	650	10
SP272	GaN	750	0
SP280	GaN	550	10
SP316	GaN	500	0
SP318	Sapphire	500	10

down to 100 μm, and then dimpling to 10 μm. The electron transparency was finally obtained by ion milling, with the sample holder kept at liquid nitrogen temperature in order to minimize the irradiation damage. The observations were carried out in a 002B Topcon high resolution microscope operated at 200 kV.

III. RESULTS

In the following, we first discuss the influence of the deposition temperature on the sputtered ZnO crystalline structure. Next, we present the results on the various phases that form upon doping the layers with Mn.

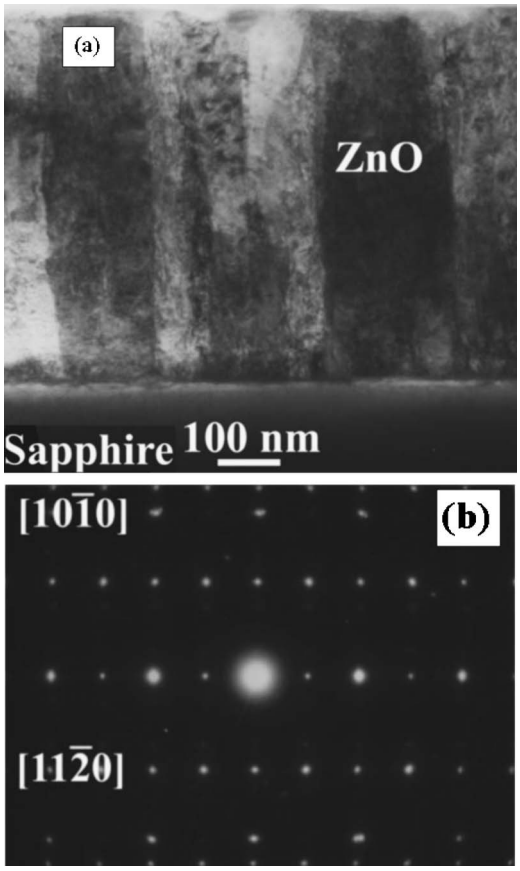

FIG. 1. (a) Large columns after deposition at 650 °C. (b) A diffraction pattern of a large area showing the two epitaxial relationships of the columns; the two coexisting zone axes are marked.

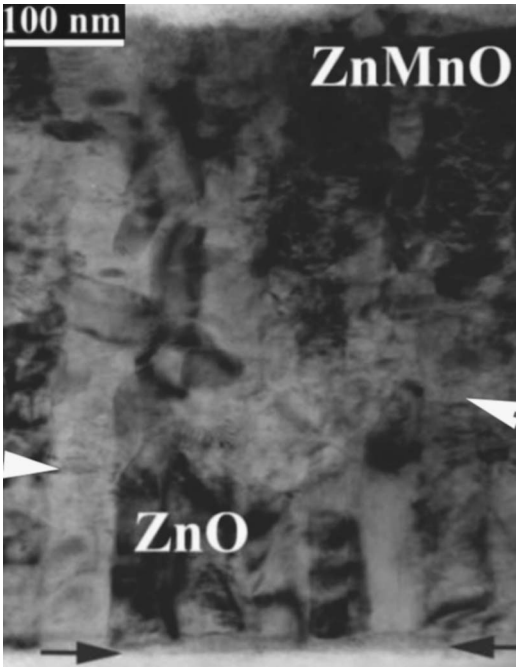

FIG. 2. Layer deposited at 550 °C: rough interface to the Mn-doped area towards the surface (white arrows) and an intermediate phase at the sapphire surface (black arrows).

A. Influence of the deposition temperature

1. The structure of the layers

The first observation is a large influence of the deposition temperature on the layer microstructure, especially on sapphire. At the highest temperatures (650 °C), the layers exhibited a strong columnar growth, with large adjacent columns (diameter $>$ 200 nm) of different orientations as can be noticed in the bright field micrograph of Fig. 1(a) in which the dark columns are imaged along the [11$\bar{2}$0] axis of ZnO. As recorded along the [10$\bar{1}$0] zone axis of sapphire, the diffraction pattern [Fig. 1(b)] in an area containing many columns in ZnO exhibits two zone axes, the [10$\bar{1}$0] and [11$\bar{2}$0]. In this diffraction pattern which is a superimposition of the two zone axis patterns, the central row belongs to the two

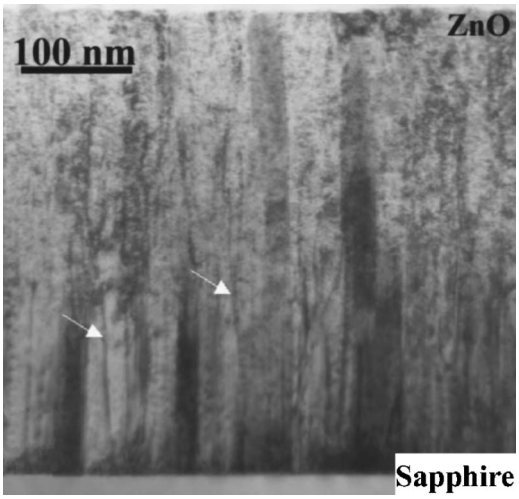

FIG. 3. Deposition at 500 °C, the layers exhibit a mosaic growth.

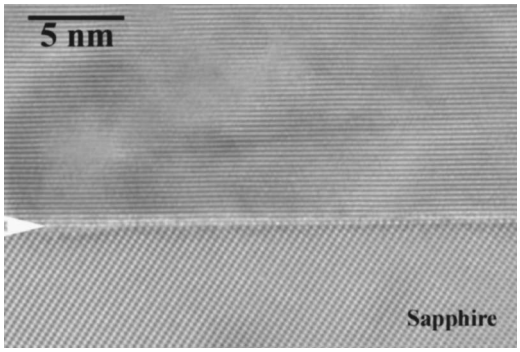

FIG. 4. A high resolution micrograph of the interfacial area with the sapphire substrate, SP316 (500 °C); the interface between ZnO and sapphire is atomically abrupt (white arrow).

zones, with the 0002*n* spots clearly underlined by the overlap. On each part, the two inner rows belong to the $[11\bar{2}0]$ zone and the next two belong to $[10\bar{1}0]$. Therefore the two main epitaxial relationships in the mismatched growth of wurtzite structures, which have been reported on the growth of wurtzite GaN on the [0001] sapphire surface,[18] coexist in these layers and adjacent columns can be rotated, one from the other, by 90° around the [0001] direction. When the deposition temperature is lowered to 550 °C, the columnar growth is still present, but the column diameter is strongly decreased; the size of the individual columns is below 50 nm (Fig. 2). In this sample, the Mn doping was 10% (Fig. 2). There is a clear structural difference between the doped and undoped areas, as can be seen (arrows); the doping was started after the deposition of about 150 nm undoped ZnO. In the undoped region, the columnar growth is still visible, whereas the doped area contains a large number of precipitates of various shapes and sizes, which blur out the columnar structure. The interface between the two areas is very rough as indicated by the two white arrows. The peak-to-peak roughness is about 40 nm substantially larger than at the top surface of the Zn(Mn)O layer. This may imply that there has been an interdiffusive reaction in this area, either during the deposition or the subsequent annealing step, which took place at 850 °C. At the interface with the sapphire substrate (see black arrows), there is a thin layer which exhibits a different contrast, and this is the case as well for the layers deposited at 650 °C.

When the deposition temperature is decreased to 500 °C, the misorientation between the growth domains becomes very small; the epitaxial relationship which dominates the growth on (0001) sapphire and also for GaN is the only one to take place.[19] The layers end up with a mosaic growth mode (Fig. 3) as has been already pointed out in GaN layers

TABLE II. Column diameter and interfacial phase formation vs the deposition temperature.

T/Sub (°C)	Sapphire (nm)	Interphase
650	200	Yes
550	60	Yes
500	~10	No

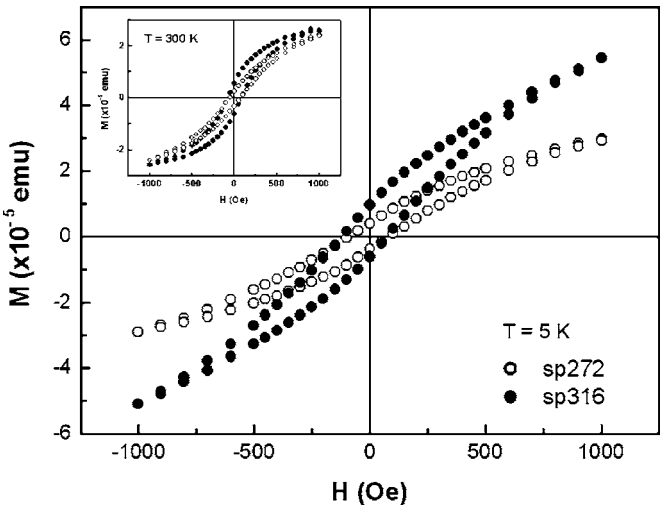

FIG. 5. Net magnetization at 5 K of samples SP272 deposited at 750 °C and SP316 deposited at 500 °C. In the insert, the net magnetization of the same samples at 300 K.

grown on top of sapphire[20] and only one epitaxial relationship is exhibited: $[0001]_{sap}\|[0001]_{ZnO}$ and $[10\bar{1}0]_{sap}\|[11\bar{2}0]_{ZnO}$. The adjacent columns are now bounded by threading dislocations; some of them are shown by arrows in Fig. 3. At the interface with the sapphire substrate, the ZnO layer has now grown directly; there is no intermediate phase as in samples deposited at higher temperatures (Fig. 4). In this high resolution TEM image, the sapphire substrate is viewed along the $[11\bar{2}0]$ zone axis. The transition between sapphire and ZnO takes place within one atomic layer as shown by the white arrow. So, as far as the ZnO layer quality is concerned, within the investigated temperature range, it appears that the best growth condition is attained at the lowest used temperature of 500 °C. At this temperature (Table II), there is no more columnar growth and no interfacial phase is formed.

2. The magnetic properties

The magnetic susceptibility was also measured for the samples deposited at various temperatures. A typical example is shown in Fig. 5 for samples SP272 and SP316, which were deposited at 750 and 500 °C, respectively. Hysteresis loop behavior is observed at both temperatures; the magnetization at 300 K is relatively weak. The magnetic signal from the sapphire substrate was subtracted in these measurements. Temperature dependent magnetization (*M* vs *T*) measurements of the Mn-doped ZnO film were performed under both zero-field-cooled (ZFC) and field-cooled (FC)

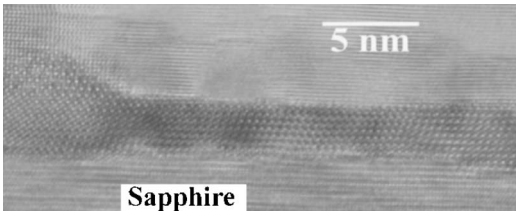

FIG. 6. A high resolution micrograph of the interfacial phase in 550 °C ZnO on (0001) sapphire.

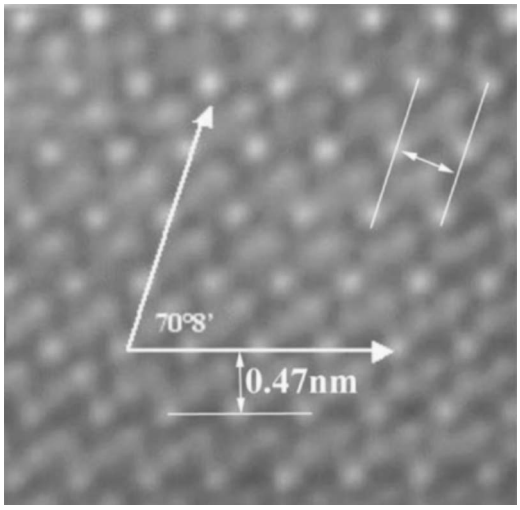

FIG. 7. A high magnification of the interfacial layer showing some equivalent spacings.

conditions and para- and diamagnetic contributions to the hysteresis loop were eliminated.[17] Thus, we conclude that the magnetization hysteresis loops are attributed to the ferromagnetism of the Mn-doped ZnO film. Ferromagnetism is exhibited for both samples at low temperature as well as at room temperature and the best magnetic characteristics are again obtained in the SP316 layer, which was deposited at 500 °C.

B. The ZnO/sapphire interfacial phase

A micrograph of the interfacial phase, which formed in the high temperature layers, is exhibited in Fig. 6. As can be noticed, the thickness of this layer is not a constant, it can extend from 2 to 5 nm. However, one point is quite obvious: there is a noticeable difference between its two interfaces. The ZnO/interphase side is abrupt within one atomic layer, whereas the interphase/sapphire interface extends to a few monolayers. This is a possible indication that the reaction, which led to its formation, may have proceeded from ZnO towards sapphire. Moreover, all over this layer, one family of lattice fringes is parallel to the (0001) sapphire. In this area, we have a crystalline phase, which is viewed along a low index zone axis. As can been seen in Fig. 7, two families of lattice planes are present in this highly magnified part of the same image and they have the same d spacing as well as an angle of 70°8′. This is a good indication that this interphase is most probably cubic.

We have carried out energy dispersive spectroscopy (EDS) analysis in this interfacial area using a beam diameter of about 3 nm; the various spectra are shown in Fig. 8. The spectra were recorded just on top of the interphase and at about 6 nm on each side. They show clearly that at this scale, there is negligible interdiffusion between sapphire and ZnO [Figs. 8(a) and 8(c)].

The most striking observation is that the interphase layer contains Mn. This means that during the deposition and most probably during the subsequent annealing process, Mn has diffused from the doped area (150 nm) and come to react at the interface with sapphire. In the first 100–150 nm undoped ZnO, independent of the position, we have not been able to

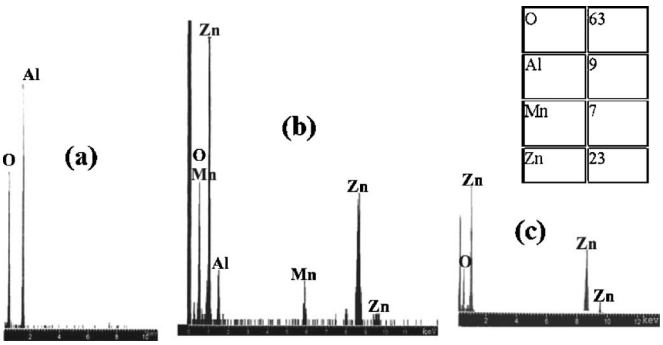

FIG. 8. EDS analysis of the interfacial area: (a) 6 nm inside sapphire, (b) on top of the interphase, and (c) 6 nm inside the ZnO.

detect any Mn. It is then possible that there has been some driving force for the reaction to take place only at the interface. In Fig. 8, we have inserted the deduced atomic composition of this phase. Although the error bars are difficult to estimate and can be important, mainly due to our experimental setup, this analysis is an indication that this compound may be a trimetallic oxide with roughly the same amount of Mn and Al.

C. The precipitates inside Mn doped areas

As can be seen in Fig. 9, numerous precipitates are present inside the Mn containing areas, particularly in this layer doped at 10%. They have various shapes and sizes and can be as large as a few hundred nanometers. Some may be elongated in the basal plane (black arrows) and others may be more or less round shaped (white arrows). As the round shaped ones are mostly of large size, we have been able to identify their structure and composition using EDS and high resolution transmission electron microscopy (HRTEM). A typical HRTEM image of a round shaped precipitate is shown in Fig. 10. At this scale, the interface of the precipitate with the surrounding matrix is formed by well defined crystallographic facets in the form of ledges separated by steps (arrows).

From Fig. 10, we can extract a number of data and useful information on the precipitate and its crystallographic relationship with the surrounding ZnO matrix. The typical angles of 110° between two equivalent directions and the 90° angle between two others allow us to identify the [110] zone axis of a cubic structure. In reference to the surrounding ZnO matrix, we measured d_{111}=4.95 Å and d_{220}=2.98 Å within 0.1 Å error. We also see clearly that one set of the (111) planes is parallel to type (0001) basal planes of ZnO. EDS

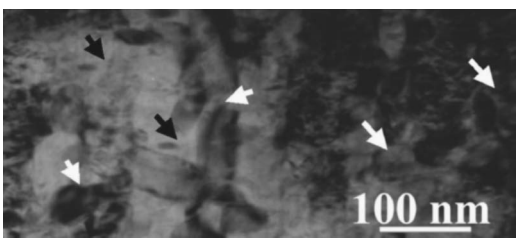

FIG. 9. Precipitation in 10% Mn-doped ZnO layer; arrows show some of the precipitates.

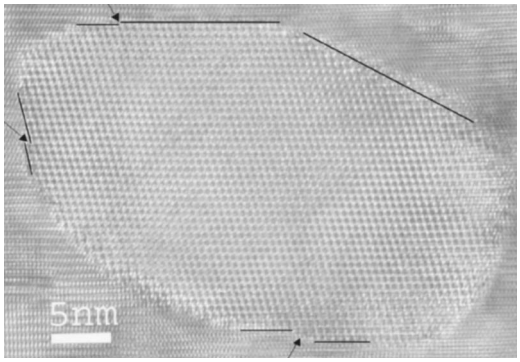

FIG. 10. A high resolution TEM micrograph of a typical cubic precipitate viewed along the [110] zone axis.

analysis (Fig. 11) of this precipitate gives a $ZnMnO_3$ stoichiometry, which agrees with these d spacings within the 0.1 Å errors as stated above. So this precipitate is of cubic symmetry with $a=8.35$ Å and $d_{111}=4.83$ Å. Along the [0001] ZnO direction, the formation of such precipitates needs the accommodation of a quite large mismatch (7%). Work is in progress to determine if the observed precipitates have any connection with the measured ferromagnetism.

IV. SUMMARY

The microstructure of Mn-doped ZnO layers obtained by rf sputtering on (0001) sapphire is presented. It is shown that for the optimum deposition temperature of 500 °C, the columnar structure is replaced by the most common mosaic growth with only one epitaxial relationship between ZnO and sapphire, and the interface between ZnO and sapphire is sharp. The Mn-doped ZnO layer exhibited round shaped cubic and elongated MnZn oxide precipitates. The round shaped precipitates are $ZnMnO_3$; they are facetted with extended (0001) ledges and coherent areas. The other type of precipitates is elongated inside the ZnO basal plane with almost the same c lattice distance. At higher deposition temperatures, a trimetallic $(AlMn)ZnO_3$ phase formed in the ZnO/sapphire interface region. In these Mn-doped layers, a magnetic effect has been measured and its highest values correspond to the optimized growth conditions. For the time being, investigation is still underway in order to determine if the formation of precipitates is to be correlated with the magnetization. However, it is clear that, even if the precipitates were not magnetic themselves, their formation may modify the local properties of the doped matrix.

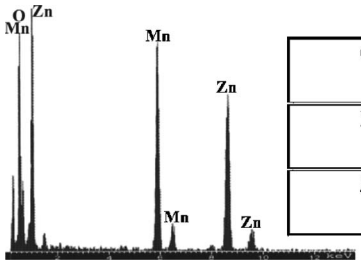

O	61
Mn	21
Zn	19

FIG. 11. The EDS analysis of the cubic precipitates and atomic composition of the cubic precipitate of Fig. 10.

[1] H. Munekata, H. Ohno, S. von Molnar, A. Segmüller, L. L. Chang, and L. Esaki, Phys. Rev. Lett. **63**, 1849 (1989).
[2] H. Ohno, A. Shen, F. Matsukura, A. Oiwa, A. Endo, S. Katsumoto, and I. Iye, Appl. Phys. Lett. **69**, 363 (1996).
[3] T. Dietl, H. Ohno, F. Matsukura, J. Cibert, and D. Ferrand, Science **287**, 1019 (2000).
[4] P. Sharma *et al.*, Nat. Mater. **2**, 673 (2003).
[5] Y. W. Heo *et al.*, Appl. Phys. Lett. **84**, 2292 (2004).
[6] S. W. Yoon, S.-B. Cho, S. C. We, S. Yoon, B. J. Suh, H. K. Song, and Y. J. Shin, J. Appl. Phys. **93**, 7879 (2003).
[7] S. W. Jung, S.-J. An, G.-C. Yi, C. U. Jung, S.-I. Lee, and S. Cho, Appl. Phys. Lett. **80**, 4561 (2002).
[8] S. Lim, M. Jeong, M. Ham, and J. Myoung, Jpn. J. Appl. Phys., Part 2 **43**, L280 (2004).
[9] S. S. Kim, J. H. Moon, B.-T. Lee, O. S. Song, and J. H. Je, J. Appl. Phys. **95**, 454 (2004).
[10] S. J. Pearton, C. R. Abernathy, D. P. Norton, A. F. Hebard, Y. D. Park, L. A. Boatner, and J. D. Budai, Mater. Sci. Eng., R. **40**, 137 (2003).
[11] V. Srikant, V. Sergo, and D. R. Clarke, J. Am. Ceram. Soc. **78**, 1931 (1995).
[12] A. P. Roth and D. F. Williams, J. Appl. Phys. **52**, 6685 (1981).
[13] B. Cockayne and P. J. Wright, J. Cryst. Growth **68**, 223 (1984).
[14] C. R. Gorla, N. W. Emanetoglu, S. Liang, W. E. Mayo, Y. Lu, M. Wraback, and H. Shen, J. Appl. Phys. **85**, 2595 (1999).
[15] A. C. Jones, S. A. Rushworth, and J. Auld, J. Cryst. Growth **146**, 503 (1995).
[16] F. Vigue, P. Vennegues, C. Deparis, S. Vezian, M. Laugt, and J.-P. Faurie, J. Appl. Phys. **90**, 5115 (2001).
[17] C. Liu *et al.*, J. Appl. Phys. **97**, 126107 (2005).
[18] Ü. Özgür, A. Teke, C. Liu, S.-J. Cho, H. Morkoç, and H. O. Everitt, Appl. Phys. Lett. **84**, 3223 (2004).
[19] K. Dovidenko, S. Oktyabrky, J. Narayan, and M. Razeghi, J. Appl. Phys. **79**, 2439 (1996).
[20] F. A. Ponce, MRS Bull. **22**, 51 (1997).